^{13}C-NMR Studies of Commercial and Partially Self-Condensed Hexakis(methoxymethyl)melamine (HMMM) Resins

RAMACHANDRAN P. SUBRAYAN and FRANK N. JONES*

Coatings Research Institute, Eastern Michigan University, 430 W. Forest Ave., Ypsilanti, Michigan 48197

SYNOPSIS

^{13}C-nuclear magnetic resonance (NMR) spectroscopy was employed to study the linkages in three commercial fully methylolated melamine–formaldehyde (HMMM) resins and their partially self-condensed resins by acid catalysis, in order to probe the structures linking melamine units. Distortionless enhancement by polarization transfer (DEPT) experiments show that the partially self-condensed resins contain both methylene ether ($\diagdown$NCH$_2$OCH$_2$N$\diagup$) and methylene ($\diagdown$NCH$_2$N$\diagup$) linkages between melamine units. The extent of these linkages were estimated by quantitative ^{13}C-NMR spectroscopy using inverse gated decoupling techniques. The results show that the ratios of methylene ether and methylene linkages to the triazine moiety vary from resin to resin. © 1996 John Wiley & Sons, Inc.

INTRODUCTION

Melamine–formaldehyde (MF) resins find several areas of applications such as lithography,[1] as a matrix in nonlinear optics,[2] and in high solids coatings[3] where they are used as crosslinkers for polymeric diols[4] and polyols.[5] MF resins also crosslink by themselves to an insoluble mass when heated in the presence of acid catalysts. This process is called self-condensation. Crosslinking of diols and polyols is also accompanied by some degree of self-condensation. Thus, the degree of self-condensation and the types of reactions involved may significantly affect the properties of the important classes of materials made from MF resins.

MF resins are synthesized by formylating melamine using a base catalyst usually followed by alkoxylation with an acid catalyst. There are several types of MF resins depending on the degrees of formylation and the degrees of alkoxylation. A completely formylated MF resin will have six methylol groups substituted at the amino nitrogens of the
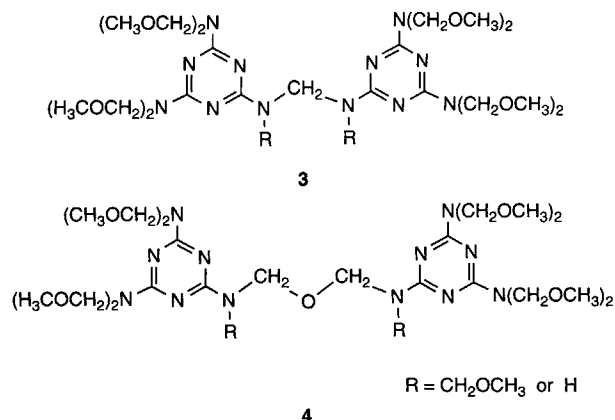
melamine with the idealized structure 1. An important commercial MF resin known as hexakis(methoxymethyl)melamine or HMMM contains a high proportion of structure 2 with the methylol groups blocked by methyl groups. It has been reported that among the MF resins the reactivity of the completely methylolated resins such as 2 with diols is greater than that of partially methylolated MF resins.[6]:
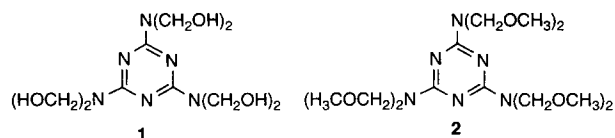
Structures 1 and 2 are only idealized structures. In reality, the resins contain dimeric, trimeric, and higher-order oligomeric structures. The reaction pathways leading to the oligomerization of these resins have been postulated in the literature.[7] These oligomers may have methylene ($\diagdown$NCH$_2$N$\diagup$) and/ or methylene ether ($\diagdown$NCH$_2$OCH$_2$N$\diagup$) linkages between the melamine groups. Idealized forms of

the dimeric structures (**3** and **4**) of HMMM resins having these linkages are shown below:

(CH₃OCH₂)₂N   N(CH₂OCH₃)₂

(H₃COCH₂)₂N   CH₂   N(CH₂OCH₃)₂
                R   R

3

(CH₃OCH₂)₂N   N(CH₂OCH₃)₂

(H₃COCH₂)₂N   CH₂   O   CH₂   N(CH₂OCH₃)₂
              R   R

R = CH₂OCH₃ or H

4

Knowledge of the structure of the self-condensation sites is desired to help understand the structure–property relationships in materials containing MF resins. The structure of MF resins have been studied by several groups. Simmonds and Dua[8] studied the reactions of (N-hydroxymethyl)-pentamethyl melamine, which can be considered as a model compound for MF resins and related compounds, using MNDO calculations and confirmed that the reactions involving the methylol group (—CH₂OH) are pH-dependent. Snyder and Vuk[7] reported that the self-condensation of HMMM is sensitive to the pH of the solution and also to the presence of alcohols added. Scheepers et al.[9] synthesized MF resins by varying the ratio of formaldehyde to melamine (F/M) and also the pH of the solution and reported their results from Raman and ^{13}C-nuclear magnetic resonance (NMR) spectroscopy and high-pressure liquid chromatography (HPLC). The results show that there is predominance of the methylene linkages ($>$NCH₂N$<$) at low pH and low formaldehyde concentrations, whereas at high pH and high formaldehyde concentrations, there is predominance of the methylene ether ($>$NCH₂OCH₂N$<$) linkages. In a separate article, they also reported the ^{1}H- and ^{13}C-NMR studies of the formation of these MF resins and concluded that both methylene and methylene–ether bridges are formed during cure.[10] More recently, Meijer et al.[11] reported the use of force-field calculations to substantiate the observations from infrared and Raman spectroscopic data for these resins. Nastke et al.[12] used polarography to study the concentration–time relationship of the reactive species in the oligocondensation of melamine with formaldehyde at pH 7–10. Their observations also

suggest that the methylol group is converted to methylene and methylene ether linkages by acid- and base-catalyzed reactions, respectively.

There are several reports of the use of NMR and mass spectroscopy for structure determination of MF resins. For example, Braun and Unvericht[13] recently studied the co-condensation of MF and phenol–formaldehyde resins using matrix-assisted laser desorption/ionization (MALDI) spectroscopy and ^{13}C-NMR spectroscopy. Starzynska et al.[14] reported the mechanism of condensation and structure of MF resins using ^{13}C-NMR, mass spectroscopy, and gel permeation chromatography (GPC) for the development of liquid adhesive compositions for wood-based materials. More recently, Andreis et al. reported solid-state ^{15}N-NMR (Ref. 15) and ^{13}C NMR (Ref. 16) studies of HMMM resins. Their data suggested that the melamine units in oligomeric HMMM resins are linked together exclusively by methylene ether linkages. In early NMR studies, at least four authors detected $>$NCH₂OCH₂N$<$ bridges but did not detect $>$NCH₂N$<$ bridges in HMMM resins or their self-condensed products.[17]

^{13}C-NMR spectroscopy can potentially provide a wealth of information such as the ratio of melamine-to-formaldehyde content, the degree of incorporation of formaldehyde as methylol groups, —CH₂— linkages, —CH₂OCH₂— linkages, and the extent of branching.[18] In 1992, we published an article regarding the ^{13}C-NMR studies of self-condensed MF resins and the possible linkages involved.[19] In these experiments, using model compounds, we concluded that among the methylene ether and methylene bridges the former is the more predominant linkage present in MF resins. The model compound studies also indicated that the methylene bridges existing in cyclic form as hexahydro-s-triazine derivatives can form and are relatively more stable than are acyclic bridges.[19,20] The steps leading to the formation of these bridges are considered to be reversible. Recently, Chang[21] reported liquid chromatography/mass spectrometry (LC/MS) studies on readily available HMMM resins. The LC/MS studies of the dimeric fraction show strong evidence for the existence of $>$NCH₂N$<$ linkages (M⁺ 704) in these resins as shown in structure **3** (R = —CH₂OCH₃). Chang's report, which seemed to contradict our 1992 results, prompted an extension of our earlier studies using ^{13}C-NMR spectroscopy.

The present study was undertaken to acquire better evidence about the prevalence of methylene and methylene ether bridges in HMMM resins before and

Table I   Physical Properties of HMMM Resins Used in This Study[a]

Code	Resin	Combined Ratio[b]	Maximum Free Formaldehyde	% Monomer Content	DP	M_n
HMMM1	Resimene 745	3.0/5.8/5.1	0.35	62	1.3	460
HMMM2	Resimene 747	3.0/5.8/5.0	0.25	67	1.4	511
HMMM3	Resimene 2612	N.A.	N.A.	N.A.	Low	N.A.

[a] Source: Product Information, Monsanto Co.
[b] Moles combined: triazine carbons/formaldehyde/methanol; N.A. = not availble.

after self-condensation. To accomplish this goal, it became necessary to assign all the peaks, including minor peaks, present in the resins and in the self-condensates, pulling together the scattered literature data concerning these assignments. We examined three commercial HMMM resins by ^{13}C-NMR spectroscopy before and after subjecting them to partial self-condensation by heating to 80–100°C in the presence of an ~ 0.02 wt % methanesulfonic acid catalyst. By trial and error, we learned to stop self-condensation before insoluble material began to separate. Thus, partially self-condensed materials with increased concentration of the bridging groups were obtained.

EXPERIMENTAL

The three HMMM resins studied here, Resimenes 745, 747, and 2612, were obtained from Monsanto. They are labeled HMMM1, HMMM2, and HMMM3, respectively. They are comparable to the HMMM resins used in Chang's LC/MS studies,[21] with Resimene 2612 (HMMM3) being the most monomeric; it is a solid (mp 36–38°C). Resimene 745 (HMMM1) is a commercially available liquid HMMM resin. Resimene 747 (HMMM2) is also a liquid HMMM resin but is said to have a slightly higher molecular weight than that of HMMM1. All these resins are expected to provide good film flexibility and toughness. Some of the properties of these resins are shown in Table I.

Self-condensed oligomeric HMMM resins were prepared according to the following procedure: Approximately 5 g of each HMMM resin was mixed with 0.01–0.03 g of methanesulfonic acid (~ 0.02 wt %) in an aluminum pan. The reaction mixture was heated for 20 min at 80–100°C on a hot plate in a stream of ordinary air to remove the volatiles. Upon heating, the liquid resin gradually turned more viscous, and at that time, the aluminum pan was removed from the hot plate and allowed to cool to room temperature to give a slightly viscous resin. The resin was left in the air stream for 4–6 h to remove most of the volatiles. Gel permeation chromatography (GPC) of the self-condensed HMMM3

was performed in a Hewlett-Packard 1050 instrument with Phenomenex 500, 500, 500, and 100 columns in series (see Fig. 1) using polystyrene standards. It showed dimeric, trimeric, and polymeric components, which is comparable to the reported data for a similar partially self-condensed HMMM resin.[22] Approximately 0.08 g of the resin was dissolved in 1 mL DMSO-d_6. These solutions were used for NMR analysis in 5 mm-diameter NMR tubes.

^{13}C-NMR (62.5 MHz) spectra were recorded using a Bruker AC-250 spectrometer. Chemical shift values are reported relative to the solvent (39.50 ppm for DMSO-d_6). The 90° pulse width was 5.9 μs and field/frequency stabilization was achieved utilizing an internal deuterium lock. Spectral width of $15K$ Hz using $32K$ data points was selected. Quadrature phase detection was used to detect the NMR signals. Spin-lattice relaxation times (T_1) were obtained using the standard inverse recovery pulse sequence ($180°$–τ–$90°$–T_R, where τ is the delay time and T_R is the repetition rate). Pulse delays of at
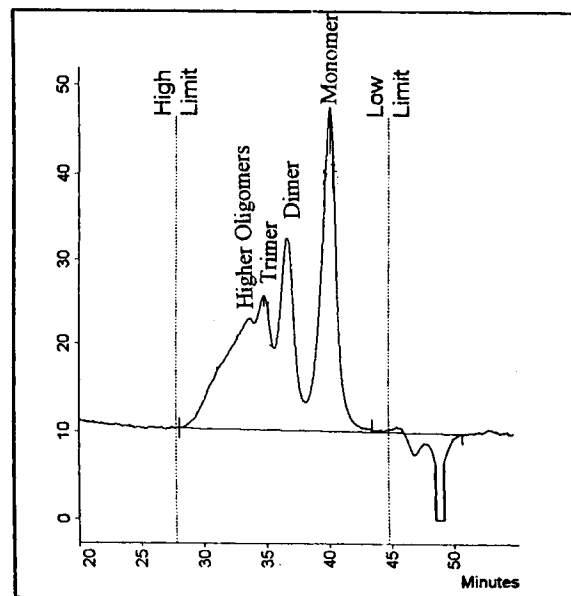
Figure 1   Gel permeation chromatography of partially self-condensed HMMM3 resin.
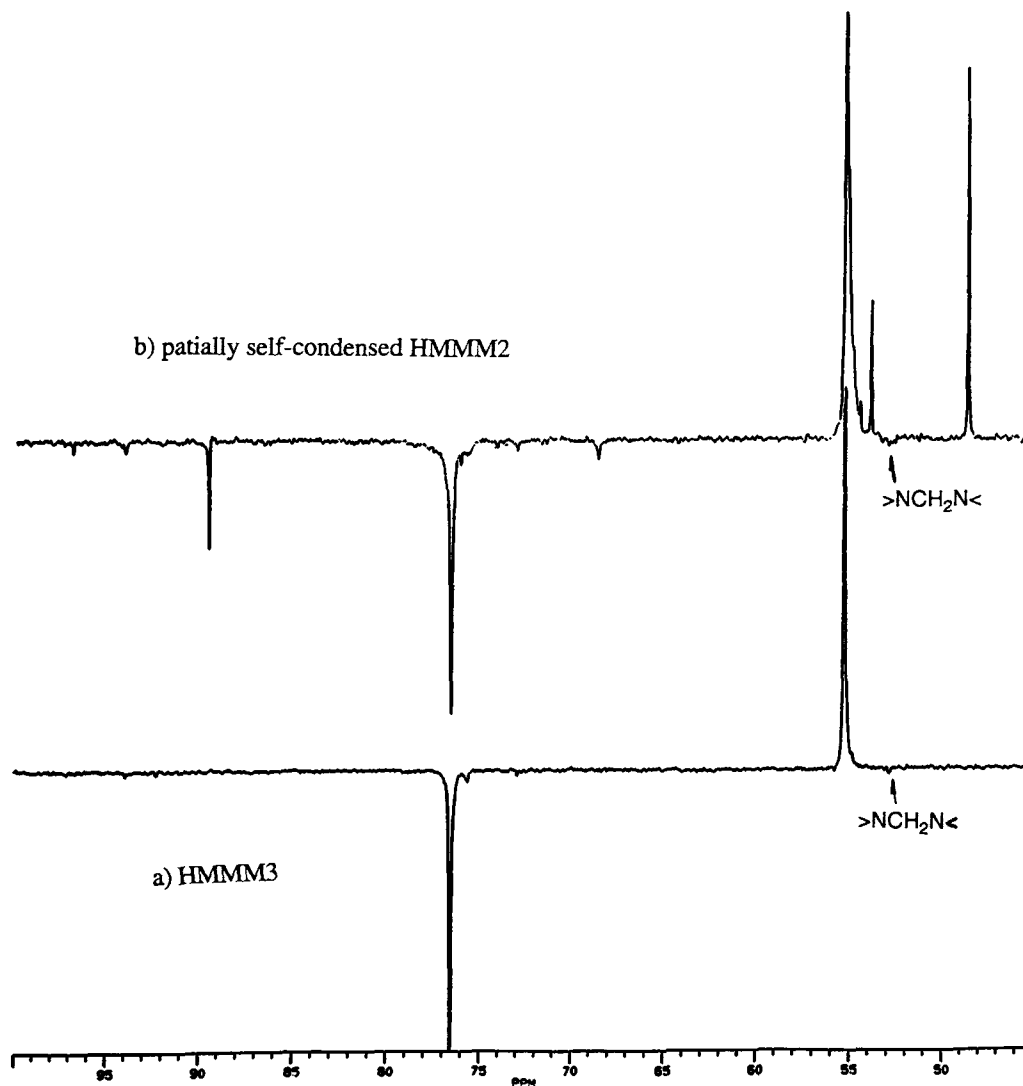
Figure 2   DEPT spectra of (a) HMMM3 and (b) partially self-condensed HMMM2.

least $5T_1$ were used between successive pulse sequences for T_1 measurements. Quantitative ^{13}C-NMR experiments were performed using inverse gated decoupling in order to suppress the nuclear Overhauser enhancement (NOE) in which the decoupler is turned on and off in the following sequence[23]: decoupler on–τ-pulse–FID acquisition–τ-decoupler off–T_R, where $\tau \ll T_R$. The delay time between pulses (τ) was 10 s. Approximately 4000 free-induction decays (FIDs) were accumulated before Fourier transformation. The experiment was run with and without doping the samples using chromium(III) acetylacetonate, $Cr(acac)_3$, a relaxation agent which allows the nuclei to relax faster and thereby suppresses the NOE effect. First-order polynomial base-line correction was used for all ^{13}C-NMR spectra before quantitation. Details about DEPT experiments are described elsewhere.[19]

RESULTS AND DISCUSSION

Our experiments were focused on highly methylolated MF resins HMMM1, HMMM2, and HMMM3, which are similar to the methylated MF resins studied by Chang.[21] Preliminary ^{13}C-NMR of HMMM3, which most closely approaches the idealized structure **2**, shows the $-OCH_3$ carbon at 55.27 ppm and $\diagdown{N}CH_2O-$ carbon at 76.49 ppm. The DEPT spectrum of HMMM3 and partially self-condensed HMMM2 also showed these signals with the one at 76.50 ppm inverted along with very small signals of $-CH_2-$ carbons as inverted peaks at 93.96, 75.65, 72.93, and 52.88 ppm (see Fig. 2). The latter resin also had inverted peaks at 96.80, 89.48, and 68.53 ppm. Assignments of these peaks are described in Tables III–V.

In addition to the peak assignments, we also wanted to estimate the relative quantities of different carbons present for all three resins using quantitative ^{13}C-NMR experiments. This is to estimate the amount of different linkages present in the oligomeric forms of the HMMM resins and, perhaps, arrive at a conclusion as to which linkages predominate in self-condensed MF resins at two stages in the self-condensation process.

Tomita and Ono[24] reported the use of ^{13}C-NMR using an inverse gated decoupling pulse sequence to estimate the melamine content in urea–melamine formaldehyde resins. Quantitative estimation using ^{13}C-NMR spectroscopy is also documented for biologically and pharmaceutically active compounds[25] and polymers.[26] Recently, quantitative ^{13}C-NMR was also used to determine the degree of branching in hyperbranched and dendritic materials.[27]

To quantitate a ^{13}C-NMR spectrum, we need to allow all carbon nuclei to relax completely before the next pulse is applied. This suppresses the NOE effect due to the hydrogens bonded to the carbons. It could be achieved by running the ^{13}C-NMR with a long delay between pulses using an inverse gated heteronuclear decoupling technique. Determination of the spin-lattice relaxation time (T_1) is required to correctly estimate the delay time which is usually set to $5T_1$. Alternately, addition of paramagnetic relaxation agents such as Cr(acac)$_3$ also help the nuclei relax faster. However, their addition is not always recommended as they may bring about side reactions.

T_1 experiments were run using inverse recovery techniques for HMMM2 and HMMM3 (see Experimental section). The T_1 relaxation times of the triazine ring carbon and $\diagdown$N—CH_2O— and —OCH_3 carbons are listed in Table II. The T_1 data for other —CH_2— groups were not determined as they are present in very low concentrations.

HMMM3 shows the lowest T_1 value for the triazine ring carbon, perhaps because it is the most monomeric form studied here. The T_1 data for various carbons in MF resins from the literature[10] show similar results. The longest T_1 relaxation time of ca. 2 justifies the use of a 10 s ($\sim 5T_1$) delay between pulses. The ^{13}C-NMR spectrum using an inverse gated decoupling pulse sequence was run with a 90° pulse and a long relaxation delay ($D1 = 10$ s). The experiments were performed for all three resins in DMSO-d_6 before and after self-condensation. These experiments were also run by doping with Cr(acac)$_3$ as the relaxation reagent. The integration results obtained in both cases were comparable, suggesting that the appropriate delay time was selected. However, the NMR samples of the self-condensed resins

Table II T_1 Data for HMMM2 and HMMM3

		T_1 (s)	
Carbon	ppm	HMMM2	HMMM3
Triazine ring C	166.21	2.12 ± 0.09	1.68 ± 0.09
$\diagdown$N—CH$_2$—O—	76.53	0.10 ± 0.03	0.10 ± 0.03
—O—CH$_3$	55.24	1.27 ± 0.07	1.36 ± 0.07

were doped with Cr(acac)$_3$ since their T_1 values were not determined and are expected to be greater than that of commercial resins, especially for the ring carbons. Approximately 4000 FIDs were accumulated before the Fourier transformation in order to obtain the peaks of the different —CH$_2$— carbons.

The NMR spectra of commercial and partially self-condensed HMMM1, HMMM2, and HMMM3 (see Figs. 3 and 4) show more than one triazine carbon, consistent with the presence of unsymmetrically substituted molecules. The assignments of these and other major peaks, listed in Tables III and IV, were carried out according to the previously reported literature data. In the following text, tentative assignments of the minor and shoulder peaks are also described.

Assignment of Carbons in Commercial and Self-condensed HMMM Resins

It may be noticed from Tables III and IV that, generally, the chemical shifts of the peaks in HMMM3 are slightly different from the other two. This may be attributed to the fact that HMMM3 is the most monomeric form studied. The discussion of peak assignments will be discussed below for the three different types of carbons present in these resins. These include triazine, —CH$_2$—, and —CH$_3$ carbons.

Assignment of Triazine Ring Carbons

The chemical shifts of the triazine carbons will be dependent on the substitution pattern on the amino groups. A general grouping reported in the literature[10,24] is as follows: carbons with primary amine ($\diagdown$C$_{/\!/}$— NH$_2$, 167.7–166.7 ppm), those with secondary amine ($\diagdown$C$_{/\!/}$— NHR, 166.7–165.7 ppm), and those with tertiary amine ($\diagdown$C$_{/\!/}$— NR$_2$, 165.4–164.4 ppm). The literature data mentioned above are reported for nonalkylated MF resins and therefore may differ from the results obtained in this experiment for the methylated MF resins.
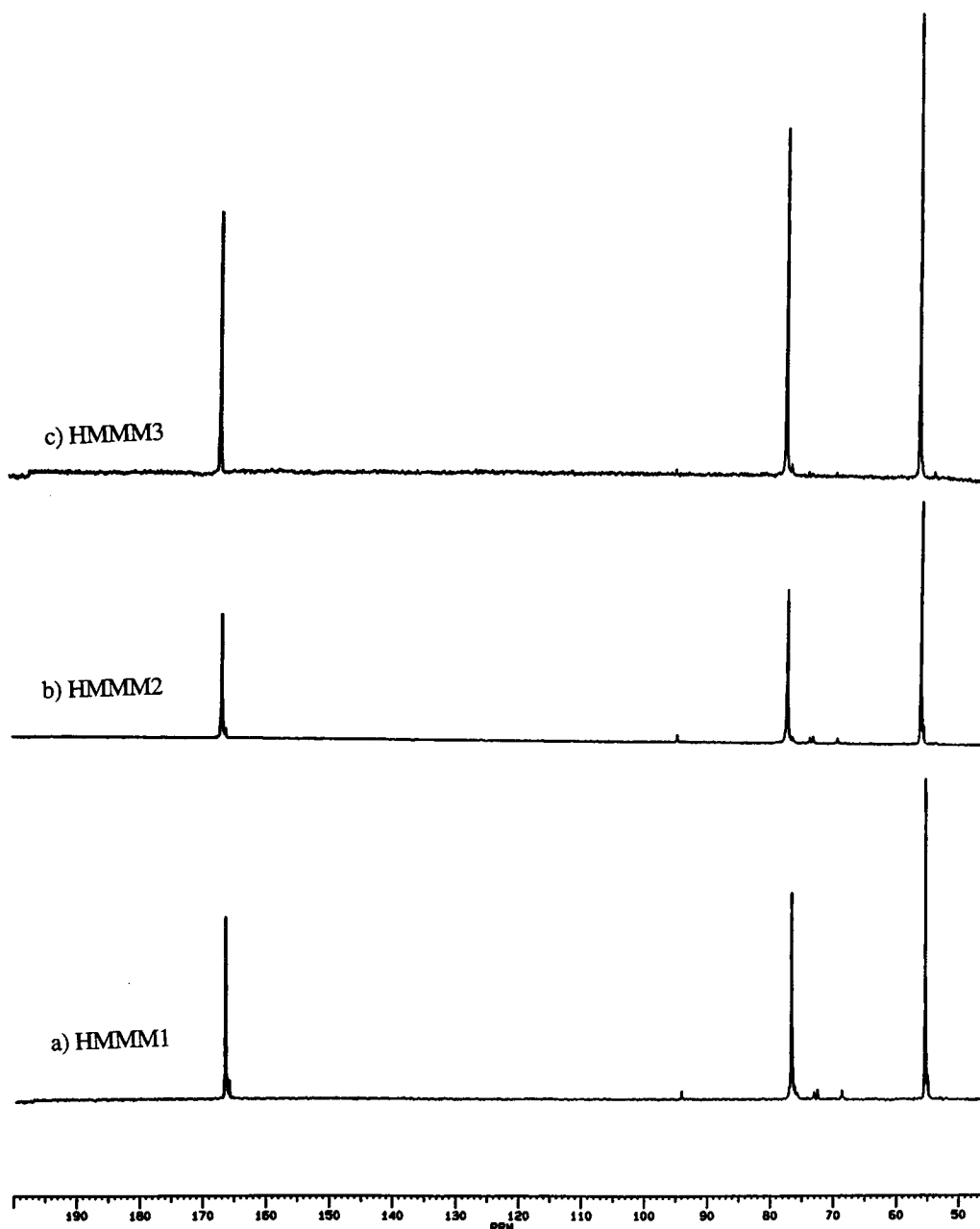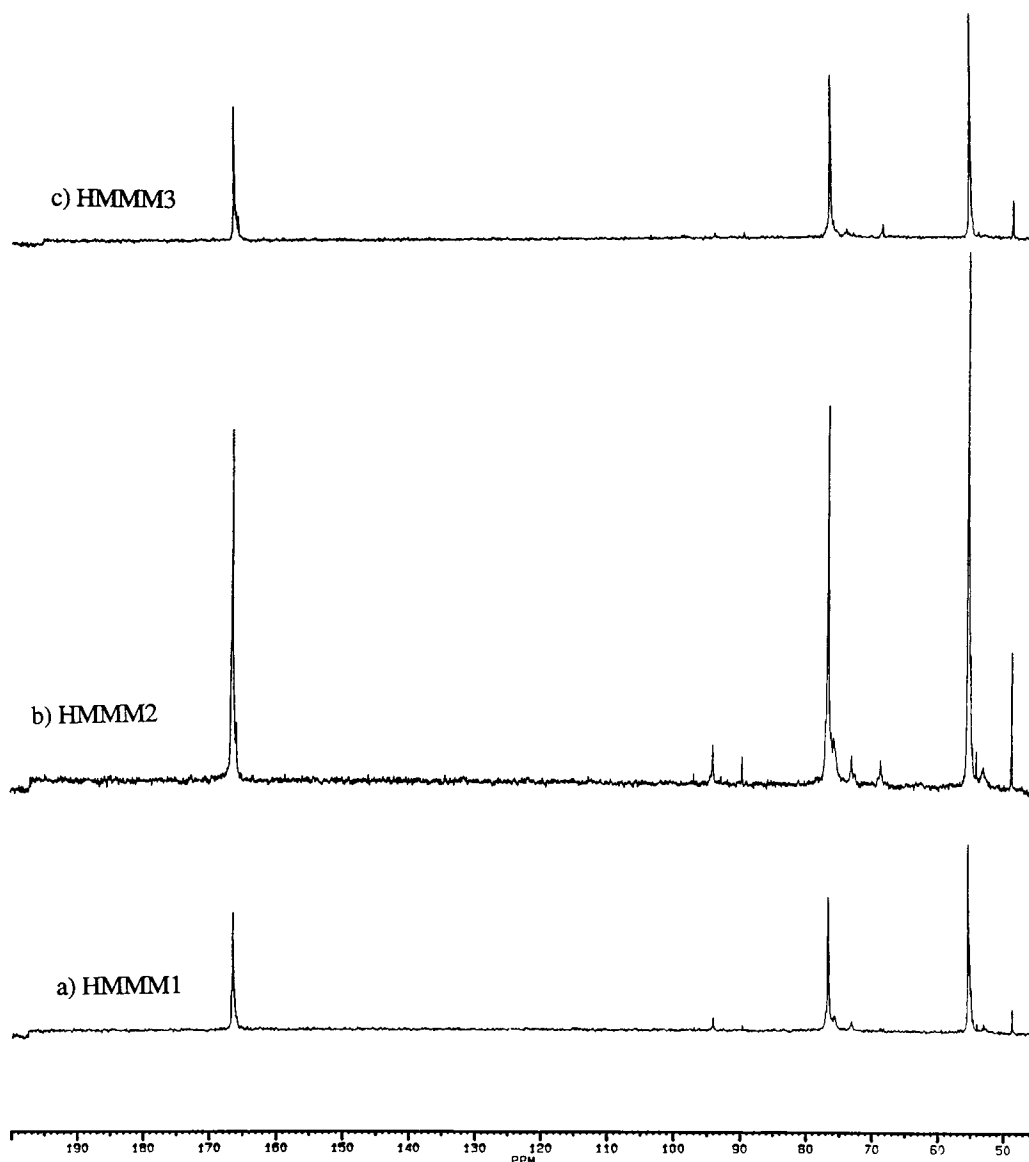
Figure 3   Inverse gated decoupled ^{13}C-NMR spectra (in DMSO-d_6) of (a) HMMM1, (b) HMMM2, and (c) HMMM3 resins.

For methylated MF resins, the trend in the triazine chemical shifts is opposite to that reported for the nonalkylated MF resins.[16] Since HMMM3 is the most monomeric, the major triazine carbon peak at 166.19 ppm must be due to the highly substituted triazine ring carbon, i.e., $\diagdown$ $\underline{C}$ — N(CH$_2$OCH$_3$)$_2$. The corresponding signal for HMMM1 and HMMM2 is at ca. 166.28 ppm. After self-condensation, this signal appears in the same range (166.25–166.29 ppm) for all three resins.

A close examination of these peaks shows an overlap of tiny signals or shoulder peaks at 166.47 and 166.09 ppm which may be due to the triazine carbons bonded to the oligomeric structures that forms methylene ether and methylene linkages in their oligomeric structures, i.e., $\diagdown$ $\underline{C}$ — N(X)(CH$_2$OCH$_3$), where X = — CH$_2$ —.

Before self-condensation, both HMMM1 and HMMM2 show a peak at 165.65 ppm, whereas after self-condensation, all three resins have a peak at

Figure 4 Inverse gated decoupled ^{13}C-NMR spectra (in DMSO-d_6) of partially self-condensed (a) HMMM1, (b) HMMM2, and (c) HMMM3 resins.

165.61–165.66 ppm as a small peak or shoulder. This peak may be assigned to the $\mathrm{\underset{/\!/}{\overset{\backslash}{C}}}$ — NH(CH_2OCH_3) carbon. This assignment is consistent with the mechanistic studies of MF resins by Blank[28] using GPC which showed that demethylolation is observed in these resins upon self-condensation.

Assignment of Methylene Carbons

MF resins have different types of methylene carbons and they appear at different chemical shifts between 45 and 100 ppm. The chemical shifts and possible assignments of these peaks in the three resins, before and after self-condensation, are discussed below.

100–89 ppm Range

The peaks between 90 and 100 ppm are generally attributed to the $- OCH_2O -$ carbons in overformylated HMMM resins or to methylol or trioxane carbons.[10,24] Before self-condensation, all three resins have a small peak at ca. 93.90 ppm which must be due to the overformylated carbon. After self-condensation, additional peaks are observed between 90 and 100 ppm. These peaks are attributed to further overformylation or due to oligomerization

Table III Chemical Shifts (ppm) and Assignments of Commercial HMMM Resins

HMMM1	HMMM2	HMMM3	Assignment
166.28	166.29	166.19	$\overset{\backslash}{\underset{/\!/}{}}\underline{C}$—N(CH$_2OCH_3$)$_2$
165.65	165.65		$\overset{\backslash}{\underset{/\!/}{}}\underline{C}$—NH(CH$_2OCH_3$)
93.94	93.94	93.89	Tr(X)NCH$_2$O$\underline{C}$H$_2$O—, HOCH$_2$O$\underline{C}$H$_2$O— or trioxane
76.56	76.55	76.49	Tr–N($\underline{C}$H$_2$OCH$_3$)$_2$
		75.58	Tr–N(X)($\underline{C}$H$_2$OCH$_2$OCH$_3$)
73.87	73.87		Tr–NH($\underline{C}$H$_2$OCH$_3$)
72.92	72.91	72.86	Tr–N(X)$\underline{C}$H$_2$OCH$_2$(X)N—Tr
72.39	72.39		Tr–N(X)$\underline{C}$H$_2$OCH$_2$NH—Tr
68.49	68.50	68.45	Tr–NH$\underline{C}$H$_2$OCH$_2$NH—
55.30	55.28	55.27	Tr–N(CH$_2$O$\underline{C}$H$_3$)$_2$
52.84	52.84	52.76	Tr(X)N—$\underline{C}$H$_2$—N(X)Tr
51.74			Tr(X)N—$\underline{C}$H$_2$—NH—Tr

Tr = 1,3,5-triazinyl; X = —CH$_2$—.

products of the liberated formaldehyde including trioxane, a cyclic trimer of formaldehyde.

The peak at 89.42 ppm, seen only after self-condensation, is assigned to CH$_3$O$\underline{C}$H$_2$OH according to the literature data.[16,20,24] Appearance of this new peak supports partial demethylolation of HMMM resins upon self-condensation.[28]

77–73 ppm Range

Before self-condensation, the strong peak observed at 76.49 ppm for HMMM3, the most monomeric of the resins, is assigned to the methylene carbon, —N($\underline{C}$H$_2$OCH$_3$)$_2$. For HMMM1 and HMMM2, it appears at ca. 76.55 ppm with shoulders at 76.86 and 76.01 ppm. The peaks at 76.86 and 76.01 ppm may be assigned to —N(X)($\underline{C}$H$_2$OCH$_3$) groups that are linked to methylene ether and methylene linkages consistent with the assignments of triazine carbon peaks in these spectra (X = —CH$_2$—).

After self-condensation, the intense peak due to the —N($\underline{C}$H$_2$OCH$_3$)$_2$ carbon appears at ca. 76.55 ppm for all three resins. The shoulder peaks at 76.86 and 76.01 ppm are still present after self-condensation.

The spectrum of HMMM3 also has a small but distinct peak at 75.58 ppm which appears at ca. 75.65 ppm as a shoulder or a weaker peak in HMMM1 and HMMM2. This may be assigned to —N(X)($\underline{C}$H$_2$OCH$_2$OR) carbon (R = H or CH$_3$) according to Tomita and Ono.[24] The peak at ca. 75.60

ppm is more resolved after self-condensation in HMMM1 and HMMM2 but is only a shoulder in HMMM3.

HMMM1 has two small but broad peaks at 74.16 and 73.87 ppm, whereas for HMMM2, only the peak at 73.87 ppm is present. These peaks are absent in HMMM3. The peak at 73.0–73.7 is assigned to the —NH$\underline{C}$H$_2$OCH$_3$ carbon by Andreis et al.[16] Schindlbauer and Anderer[29] assigned the peak at 74.3 ppm in DMSO-d_6 to the —NH$\underline{C}$H$_2$O— carbon.[†] In our study, the peak at 74.16 ppm might be tentatively assigned to the overformylated carbon, NH$\underline{C}$H$_2$OCH$_2$OCH$_3$, to be consistent with the observed overformylation.

After self-condensation, the 74.16 and 73.87 ppm peaks of HMMM1 have almost disappeared, whereas for HMMM2, a small but broad peak has appeared at 74.16 ppm. After self-condensation, HMMM3 has a new peak at 73.98 ppm.

73–70 ppm Range

The ^{13}C-NMR spectra of HMMM1 and HMMM2 show two distinct peaks at 72.91 and 72.39 ppm. The intensity of these signals in HMMM3 appeared to be much weaker. After self-condensation, these peaks appear as a broad or distinct peak at ca. 72.93 ppm. Often, this peak has a shoulder at ca. 72.40

[†] Their assignment was relative to the DMSO-d_6 peak at 41.8 ppm instead of at 39.5 ppm.

Table IV   Chemical Shifts and Assignments for Partially Self-condensed HMMM Resins

HMMM1	HMMM2	HMMM3	Assignment
166.25	166.29	166.25	$\diagdown$C—N(CH$_2$OCH$_3$)$_2$
		165.96	
165.61	165.66	165.62	$\diagdown$C—NH(CH$_2$OCH$_3$)
		98.83	
96.75	96.78		Tr(X)NCH$_2$O(CH$_2$O)$_n$—,
93.91	93.94	93.92	HOCH$_2$O(CH$_2$O)$_n$— or
	92.69		trioxane
89.42	89.46	89.44	CH$_3$OCH$_2$OH
		77.10	
76.52	76.56	76.54	Tr-N(CH$_2$OCH$_3$)$_2$
75.56	75.62	75.57	Tr-N(X)(CH$_2$OCH$_2$OCH$_3$)
		73.98	Tr-NH(CH$_2$OCH$_3$)
72.90	72.93	72.91	Tr-N(X)CH$_2$OCH$_2$(X)N—Tr
	72.40		Tr-N(X)CH$_2$OCH$_2$NH—Tr
68.42	68.49	68.45	Tr-NHCH$_2$OCH$_2$NH—Tr
55.28	55.31	55.30	Tr-N(CH$_2$OCH$_3$)$_2$
53.87	53.90	53.88	Tr-NH(CH$_2$OCH$_3$)
52.84	52.87	52.83	Tr-N(X)CH$_2$(X)N-Tr
48.57	48.60	46.91	CH$_3$OCH$_2$OH or CH$_3$OH

Tr = 1,3,5-triazinyl; X = —CH$_2$—.

ppm. Since this peak grows during self-condensation, it is reasonable to assign the peak at ca. 72.93 ppm to the $\diagup$NCH$_2$OCH$_2$N$\diagdown$ carbon. This assignment is consistent with that of Braun and Unvericht[13] who assigned the peak at 72.2 ppm in MF resins (in pyridine-d_5) to the methylene ether linkage. The shoulder at ca. 72.40 ppm may be assigned to $\diagup$NCH$_2$OCH$_2$NH— carbon.

69–68 ppm Range

Before self-condensation, both HMMM1 and HMMM2 show a peak at ca. 68.50 ppm which appears as a very, very small peak at 68.45 ppm for HMMM3. This peak is attributed to —NHCH$_2$. OCH$_2$NH— carbon by Tomita and Ono[24] and Tomita and Hse.[30] After self-condensation, its intensity has significantly increased in HMMM2 and HMMM3, whereas this peak has almost disappeared in HMMM1.

Another group that might be present is the hemiacetalized methylol group. Tomita and Hse[30] reported the chemical shift of the $\diagdown$NCH$_2$OCH$_2$OH carbon to be ca. 85 ppm in DMSO-d_6. Absence of such a peak in our spectra indicates that concentration of the hemiacetalized methylol group is too low to detect, supporting the assignment of the 68.50 ppm peak to methylene ether (—NHCH$_2$OCH$_2$NH—) bridges.

53–52 ppm Range
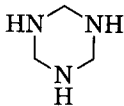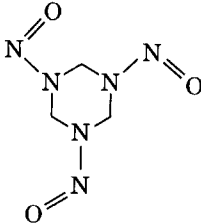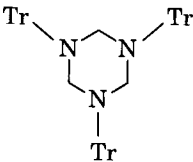
DEPT spectra showed that the small, broad peak, or cluster of peaks, at 52.88 ppm arise from —CH$_2$— carbons; they can be attributed to the methylene bridge ($\diagdown$NCH$_2$N$\diagup$) structures. Based on what is known about the chemistry of HMMM resins,[19–22] it is expected that methylene bridges with —N(X)CH$_2$N(X)— structures (X = —CH$_2$—) would predominate and that —NHCH$_2$N(X)— structures might also be present in detectable concentrations. We assign the peak(s) centered at 52.88

ppm in HMMM1–HMMM3 and at 52.83–52.87 ppm in the self-condensed resins to methylene bridges of these types.

It should be noted that the literature only partly supports this assignment. In four studies cited by Bauer[17] and in recent reports by Andreis et al.,[15,16] methylene bridges were not detected at all. However, their detection in a number of other studies[9,10,12,24,30] establish their presence, at least in unalcoholated MF resins, and Chang[21] provided strong evidence of their existence in methylolated MF resins. We could not find literature reports of chemical shifts of acyclic $\diagdown$N$\underline{\text{C}}$H$_2$N$\diagup$ structures. In cyclic hexahydro-s-triazine structures, reported chemical shifts of the $\diagdown$N$\underline{\text{C}}$H$_2$N$\diagup$ carbons range from 52.24 to 61.6 ppm, as shown in Table V.[19,31] The compound which most closely resembles the structures in HMMM resins has a peak at 52.24 ppm, consistent with our assignments. On the other hand, in studies of unalcoholated urea formaldehyde (UF), melamine formaldehyde (MF), and mixed UF–MF resins, Tomita and Ono[24] and Tomita and Hse[30] assigned peaks ranging from 47 to 60 ppm to $\diagdown$N$\underline{\text{C}}$H$_2$N$\diagup$ bridges, with —NH$\underline{\text{C}}$H$_2$NH— carbons at 46.7–49.0 ppm, —NH$\underline{\text{C}}$H$_2$N(X)— carbons at 53.1–53.8 ppm, and the N(X)CH$_2$N(X)— carbons at 59.5–60.0 ppm; the latter assignment was based entirely on unalcoholated UF-containing resins, and its applicability to HMMM resins is doubtful. Scheepers et al.[10] assigned peaks at about 48.5 and 51.5 ppm to —NH$\underline{\text{C}}$H$_2$NH— and —NH$\underline{\text{C}}$H$_2$N(X)— bridges, respectively, again in unmethylolated MF resin self-condensates. Our spectra do not have appreciable peaks in the 56–61 ppm range. It is difficult to account for the 52.8–52.9 peaks in our spectra unless they are —N(X)$\underline{\text{C}}$H$_2$N(X)— and possibly —NH$\underline{\text{C}}$H$_2$N(X)— bridges. It remains possible that peaks of some types of methylene bridge structures are masked by the strong —OCH$_3$ peaks at 53.8 and 55.3 ppm.

It is possible that the HMMM resins and especially their self-condensates could have —N(X)$\underline{\text{C}}$H$_2$N(X)— groups in acyclic structures (as in structure 3) and/or in hexahydro-s-triazine structures (as in Table V). Chang's study[21] showed acyclic bridges in the resins, and model compound studies[19,20] indicate that hexahydro-s-triazine structures could form. The question of whether cyclic structures form may have an important bearing on the stability of materials made from MF resins, but it is not answered by the present data.

Table V Chemical Shifts of the $\diagup$N$\underline{\text{C}}$H$_2$N$\diagdown$ Groups in Selected Hexahydro-s-Triazines

Compound	Chemical Shift (ppm)
	61.6[a]
	55.4[a]
	52.24[b]

Tr = bis(4,6-dimethylamino)-1,3,5-triazinyl.
[a] Ref. 31.
[b] Ref. 19.

Assignment of Methoxy Carbons

According to the DEPT studies, methyl groups appear at ca. 55.30 ppm. The strong peak at 55.30 ppm is present in all three resins before and after self-condensation. This may be assigned to the —N(CH$_2$O$\underline{\text{C}}$H$_3$)$_2$ carbons. There is also a small peak at 54.83 ppm and a weaker peak at ca. 53.89 ppm with variable intensity in all three resins. After self-condensation, only the 55.30 and 53.89 ppm peaks are distinctly observed for all three resins; the latter may be assigned to the —NHCH$_2$O$\underline{\text{C}}$H$_3$ carbon.

The 54.83 ppm peak may be assigned to the —N(X)(CH$_2$O$\underline{\text{C}}$H$_3$) carbon with $X \neq$ H or —CH$_2$OCH$_3$. After self-condensation, a new shoulder appears for HMMM1 and HMMM2 at ca. 54.45 ppm, perhaps attributable to methyl groups of higher oligomers.

Self-condensation brings about a new signal at 46–49 ppm for all three resins. DEPT spectra show this to be a CH$_3$-type carbon. This peak might be attributable to $\underline{\text{C}}$H$_3$OCH$_2$—OH or $\underline{\text{C}}$H$_3$OH carbons.

Determination of the Ratios of Various Types of Carbons

To determine the ratios of various carbons present, the areas of each peak were determined by integra-

tion using inverse gated decoupling. The area of all the peaks were normalized by setting all the triazine carbon signals to three carbons. Tables VI and VII list the areas of various carbons in different chemical shift range for commercial and self-condensed resins.

From the areas of various peaks in Tables VI and VII, the ratio of different carbons present per triazine in these resins were calculated. The areas of overformylated methylene carbons between 89 and 100 ppm and that of the $\underline{C}H_3OH$ or $\underline{C}H_3OCH_2OH$ carbons at 48–49 ppm were excluded for this purpose. The results are shown in Table VIII.

The triazine ring $C/CH_2/CH_3$ ratios for the HMMM1 and HMMM2 appear to be in fair but not perfect agreement with the literature data from Monsanto (see Table I). This may be due either to the differences in different batches or to the inherent inaccuracies of the measurement methods. HMMM3 has higher CH_3 groups per triazine present, thereby confirming its high monomer content.

The data in the last column of Table VIII shows that demethylolation occurs during self-condensation, which is consistent with Blank's evidence of demethylolation during self-condensation.[28] According to Blank's studies, the presence of water and high baking temperatures promote demethylolation and elimination of methanol. The amount of water present in the HMMM resins studied will depend on several factors including temperature and humidity. No attempt was made here to estimate the water content of these resins before, during, and after self-condensation. Evidence for demethylolation was also reported by English et al.[32] in the degradation studies of crosslinked MF–acrylic pigmented systems using solid-state NMR studies.
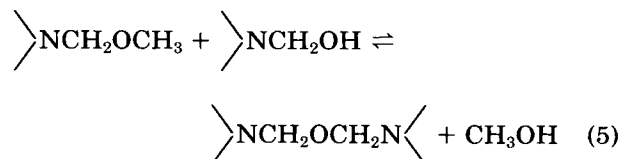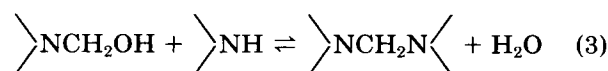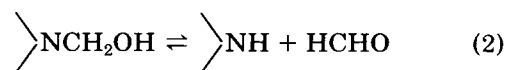
Table VI Normalized Areas of Carbons in HMMM Resins

Chemical Shift Range (ppm)	HMMM1	HMMM2	HMMM3
165.65–166.29	3.00	3.00	3.00
93.89–93.94	0.16	0.19	0.13
76.49–76.56	4.94	4.82	5.38
75.58	—	—	0.28
73.87	0.06	0.09	—
72.86–72.92	0.16	0.16	0.07
72.39	0.20	0.22	—
68.45–68.50	0.28	0.23	0.03
55.27–55.30	5.39	5.32	5.65
52.76–52.84	0.08	0.22	0.08
51.74	0.05	—	—

Table VII Normalized Areas of Partially Self-condensed HMMM Resins

Chemical Shift Range (ppm)	HMMM1	HMMM2	HMMM3
165.61–166.25	3.00	3.00	3.00
98.83	—	—	0.08
96.75–96.78	0.37	0.03	—
93.91–93.94	0.07	0.31	0.13
92.69	—	0.08	—
89.42–89.46	0.10	0.08	0.07
77.10	—	—	0.29
76.52–76.56	3.54	3.20	3.98
75.56–75.62	0.78	0.79	0.35
73.98	—	—	0.33
72.90–72.93	0.44	0.24	0.14
72.40	—	0.12	—
68.42–68.49	0.16	0.28	0.30
55.28–55.31	4.53	4.06	4.62
53.87–53.90	0.07	0.16	0.08
52.83–52.87	0.27	0.36	0.01
46.91–48.57	0.14	0.26	0.28

The methylene and methylene ether bridges are probably formed from the amines $(\!\!>\!\!NH)$ and methylols $(\!\!>\!\!NCH_2OH)$ already present and generated by the acid-catalyzed demethylolation and elimination of methanol according to the acid-catalyzed reaction schemes shown below[28]:

$$>\!\!NCH_2OCH_3 + H_2O \rightleftharpoons$$

$$>\!\!NCH_2OH + CH_3OH \quad (1)$$

$$>\!\!NCH_2OH \rightleftharpoons \;>\!\!NH + HCHO \quad (2)$$

$$>\!\!NCH_2OH + \;>\!\!NH \rightleftharpoons \;>\!\!NCH_2N\!\!< + H_2O \quad (3)$$

$$2 >\!\!NCH_2OH \rightleftharpoons \;>\!\!NCH_2OCH_2N\!\!< + H_2O \quad (4)$$

$$>\!\!NCH_2OCH_3 + \;>\!\!NCH_2OH \rightleftharpoons$$

$$>\!\!NCH_2OCH_2N\!\!< + CH_3OH \quad (5)$$
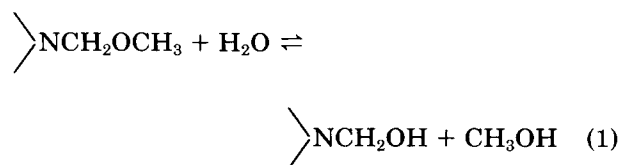
**Table VIII Combined Ratio of Triazine Ring
C/CH₂/CH₃ in HMMM Resins**

Resins	Before Self-condensation	After Self-condensation
HMMM1	3.00/5.77/5.39	3.00/5.19/4.60
HMMM2	3.00/5.74/5.32	3.00/4.99/4.22
HMMM3	3.00/5.84/5.65	3.00/5.11/4.70

All these reactions are reversible and therefore the actual amount of the formation of a specific product will depend on complex kinetic factors influenced by pH, the initial rate of heating, humidity, and the actual temperature inside the resin, etc.

From the areas of the methylene ether ($\overset{\diagdown}{\diagup}$NCH₂OCH₂N$\overset{\diagup}{\diagdown}$) linkages at ca. 72.9 ppm to that of methylene ($\overset{\diagdown}{\diagup}$NCH₂N$\overset{\diagup}{\diagdown}$) bridges at 52.8 ppm per triazine moiety, one could determine which linkages are more favored upon self-condensation. The following condition was chosen in making the calculation: Only half the area of the methylene ether bridge at 72.39 ppm ($\overset{\diagdown}{\diagup}$NCH₂OCH₂N$\overset{\diagup}{\diagdown}$) per triazine was considered toward determining the ratios since there are two methylene groups per ether linkage. However, we have not taken other methylene ether linkages (at 72.3 and 68.5 ppm) into consideration, for simplicity. The results are shown in Table IX.

The data in Table IX show that both $\overset{\diagdown}{\diagup}$NCH₂N$\overset{\diagup}{\diagdown}$ and $\overset{\diagdown}{\diagup}$NCH₂OCH₂N$\overset{\diagup}{\diagdown}$ bridges are present in commercial HMMM resins in variable amounts. Self-condensation tends to decrease the $\overset{\diagdown}{\diagup}$NCH₂OCH₂N$\overset{\diagup}{\diagdown}$ to $\overset{\diagdown}{\diagup}$NCH₂N$\overset{\diagup}{\diagdown}$ ratio for HMMM1 and HMMM2 and to increase it for HMMM3. This result suggests that both linkages are formed at different rates which are very sensitive to experimental conditions.

¹³C-NMR Studies on Aged Self-Condensed HMMM Resins

The partially self-condensed HMMM resins, which were initially slightly viscous liquids, became solid in a week, indicating that further self-condensation reactions took place at ambient temperatures. To understand the nature of these self-condensation reactions, ¹³C-NMR of the previously prepared NMR solutions in DMSO-d₆ were again run for

HMMM2 and HMMM3, approximately 1 month after. However, a new solution was prepared for HMMM1 using the previously self-condensed HMMM1 resin by stirring the resin for more than 24 h in DMSO-d₆ at room temperature and filtering the insolubles. The results are shown in Figure 5 and summarized in Table X.

The NMR spectra show a remarkable decrease in the intensities of the oligomeric formaldehyde peaks between 90 and 100 ppm but an increase in the intensities of the CH₃OCH₂OH (89.43 ppm) and CH₃OH (48.57 ppm) carbons. These observations indicate further formation of methylals and methanol.

Generally, all other carbon signals have broadened out considerably. This is more prevalent in the —N(X)CH₂— carbon signals between 70 and 75 ppm. These peaks appeared to have broadened considerably for HMMM2 and to a lesser extent in the other two resins. There is also an increase in the relative intensity of the —NHCH₂OCH₃ carbon (53.95 ppm).

The triazine carbon signals appear more or less similar for HMMM2 and HMMM3 self-condensates. For HMMM1, two equally intense triazine carbon peaks appear at 166.32 and 165.68 ppm, suggesting considerable demethylolation, perhaps during the dissolution in DMSO-d₆. While the relative intensity of the —NHCH₂OCH₂NH— carbon (68.57 ppm) increased, the $\overset{\diagdown}{\diagup}$NCH₂N$\overset{\diagup}{\diagdown}$ signal (ca. 52.8 ppm) broadened significantly. The broadness might indicate a lack of resolution in the magnetic field used or due to incipient gelation which might increase the relaxation rate of the $\overset{\diagdown}{\diagup}$NCH₂N$\overset{\diagup}{\diagdown}$ carbons in the higher oligomers. Consequently, it would be fruitless to measure the areas of these peaks.

Besides the peaks already discussed, a new peak has appeared at ca. 144 ppm for the HMMM2 self-condensate. This might be attributed to an imino (—N=CH₂) carbon. Such imino carbons can arise from —NHCH₂OCH₃ groups by acid-catalyzed elimination of methanol and subsequent deproton-

Table IX Ratio of $\overset{\diagdown}{\diagup}$NCH₂OCH₂N$\overset{\diagup}{\diagdown}$ (72.9 ppm) to $\overset{\diagdown}{\diagup}$NCH₂N$\overset{\diagup}{\diagdown}$ (52.8 ppm) in HMMM Resins

Resins	Before Self-condensation	After Self-condensation
HMMM1	1.00/1.0	0.81/1.0
HMMM2	0.36/1.0	0.33/1.0
HMMM3	0.44/1.0	7.00/1.0

Figure 5   Inverse gated decoupled ^{13}C-NMR spectra (in DMSO-d_6) of aged, self-condensed (a) HMMM1, (b) HMMM2, and (c) HMMM3 resins.

ation. Holmberg[33] studied the low-temperature acid-catalyzed self-condensation of methylated MF resins, with a high concentration of —NHCH$_2$OCH$_3$ per triazine, using ^{1}H- and ^{13}C-NMR spectroscopy in DMSO-d_6. He observed the methylene imino group at 5.2 ppm in the ^{1}H-NMR spectrum and at ca. 144 ppm in the ^{13}C-NMR spectrum. A mechanism has been proposed for its formation which is shown below:

—N=CH$_2$ + CH$_3$OH + H$_3$O$^+$

Imino groups can undergo self-condensation by two reaction pathways: (1) by trimerization to give

hexahydro-s-triazine derivatives[19,20] as discussed above and (2) by reaction with amino or methylol groups to give methylene and methylene ether linkages, respectively, as shown below. Recently, Giumanini et al.[34] also reported the formation of hexahydro-s-triazine derivatives by the thermal trimerization of the imino group in 4-methylidene-aminoantipyrine.

Formation of the imino groups during the self-condensation of fully methylolated HMMM resins has not been reported so far. The probable detection of the imino group in the NMR spectrum (Fig. 5 and Table X) suggests the possible secondary self-condensation reaction sequences shown below, besides those already discussed above:

Table X   Chemical Shifts of Partially Self-Condensed HMMM Resins After 1 Month

HMMM1	HMMM2	HMMM3	Assignment
166.32	166.27	166.27	$\underline{C}$—$N(CH_2OCH_3)_2$
165.68	165.64	165.64	$\underline{C}$—$NH(CH_2OCH_3)$
	144.00		—N=CH_2
96.82	96.77	93.94	$NCH_2O\underline{C}H_2O$—, $HOCH_2O\underline{C}H_2O$— or Trioxane
93.84	93.93		
89.50	89.46	89.44	$CH_3O\underline{C}H_2OH$
76.58	76.55	76.54	—$N(\underline{C}H_2OCH_3)_2$
68.57	68.49	68.46	—$NH\underline{C}H_2OCH_2NH$—
55.33	55.28	55.28	—$N(CH_2O\underline{C}H_3)_2$
54.33	54.45	54.82	
53.87	53.87	53.86	—$NH(CH_2O\underline{C}H_3)$
52.57	52.86	52.82	$N\underline{C}H_2N$
48.65	48.58	46.57	$\underline{C}H_3OCH_2OH$, $\underline{C}H_3OH$

In summary, specific circumstances apparently determine whether methylene ether (NCH_2OCH_2N) or methylene (NCH_2N) bridges predominate in MF resins as manufactured and in self-condensates. Thus, the apparent contradictions between our earlier study,[19] which found mainly methylene ether linkages in model compound studies, and Chang's report[21] that methylene linkages predominate can be explained. Much further research, especially kinetic studies, will be needed to fully understand the factors that govern the types of bridges formed and their effect on properties.

REFERENCES

1. E.g., see (a) I. von Lampe, M. Reinhardt, H. J. Lorkowski, and W. Schnabel, *Angew. Makromol. Chem.*, **214**, 197 (1994). (b) M. Barra, J. C. Scaiano, G. S. Calabrese, R. Sinta, and J. Thackeray, *Chem. Mater.*, **6**, 724 (1994). (c) Y. Ueda, N. Takeyama, H. Ueki, N. Takehiro, and Y. Nakano, *Can. Pat.* CA 2,100,392 (1994); *Chem. Abstr.*, **121**, 191349 (1994).

2. R. J. Jeng, G. H. Hsiue, J. I. Chen, S. Marturunkakul, L. Li, X. L. Jiang, C. Masse, J. Kumar, and S. K. Tripathy, *Mater. Res. Soc. Symp. Proc.*, **328**, 583 (1994).

3. E.g., see (a) S. Avci, N. M. Patel, L. Di Leo, and R. H. Reiter, U.S. Pat. 5,312,877 (1993); *Chem. Abstr.*, **121**, 20775 (1994). (b) W. F. Lee, *J. Appl. Polym. Sci.*, **4**, 61 (1993).

4. (a) S. M. Aharoni and S. F. Edwards, *Advances in Polymer Science*, Springer-Verlag, Berlin, 1994, Vol. 118, p. 16. (b) G. Chu and F. N. Jones, *J. Coat. Tech.*, **65**(819), 43 (1993).

5. (a) F. N. Jones, G. Chu, and U. Samaraweera, *Prog. Org. Coat.*, **24**, 189 (1994). (b) M. G. Lazzara, *J. Coat. Tech.*, **56**(710), 19 (1984). (c) G. Haacke, J. S. Brinen, and P. J. Larkin, *J. Coat. Tech.*, **67**(843), 29 (1995).

6. U. Samaraweera, S. Gan, and F. N. Jones, *J. Appl. Polym. Sci.*, **45**, 1903 (1992).

7. D. M. Snyder and T. J. Vuk, *J. Appl. Polym. Sci.*, **46**, 1301 (1992).

8. R. J. Simmonds and G. Dua, *J. Chem. Soc. Perkin Trans. 2*, 469 (1995).

9. M. L. Scheepers, J. M. Gelan, R. A. Carleer, P. J. Adriaensens, D. J. Vanderzande, B. J. Kip, and P. M. Brandts, *Vibrat. Spectrosc.*, **6**, 55 (1993).

10. M. L. Scheepers, P. J. Adriaensens, J. M. Glean, R. A. Carleer, D. J. Vanderzande, N. K. de Vries, and P. M. Brandts, *J. Polym. Sci. Part A Polym. Chem.*, **33**, 915 (1995).

11. R. J. Meijer, A. Tiller, and S. A. M. Vanhommerig, *J. Phys. Chem.*, **99**, 5457 (1995), and references therein.

12. R. Nastke, K. Dietrich, G. Reinisch, G. Rafler, and H. Gajewski, *J. Macromol. Sci.-Chem. A,* **23,** 579 (1986).

13. D. Braun and R. Unvericht, *Angew. Makromol. Chem.,* **226,** 183 (1995).

14. K. Starzynska, J. Mazur, H. Otwinowska, and A. Krystosik, *Polimery,* **37,** 25 (1992); *Chem. Abstr.,* **117,** 70776 (1993).

15. M. Andreis, J. L. Koenig, M. Gupta, and S. Ramesh, *J. Polym. Sci. Part B Polym. Phys.,* **33,** 1449 (1995).

16. M. Andreis, J. L. Koenig, M. Gupta, and S. Ramesh, *J. Polym. Sci. Part B Polym. Phys.,* **33,** 1461 (1995).

17. D. R. Bauer, *Prog. Org. Coat.,* **14,** 193 (1986), and references therein. Also see F. N. Jones, G. Chu, and U. Samaraweera, *Prog. Org. Coat.,* **24,** 189 (1994).

18. For a general review on the application of NMR spectroscopy to cross-linked polymer systems, see M. Andreis and J. L. Koenig, *Advances in Polymer Science,* Springer-Verlag, Berlin, 1989, Vol. 89, pp. 69–160.

19. U. Samaraweera and F. N. Jones, *J. Coat. Tech.,* **64**(804), 69 (1992).

20. Z. W. Wicks, Jr. and D. Y. Y. Hsia, *J. Coat. Tech.,* **55**(702), 29 (1983).

21. T. T. Chang, *Anal. Chem.,* **66,** 3267 (1994).

22. Z. W. Wicks, Jr., F. N. Jones, and S. P. Pappas, in *Organic Coatings,* John Wiley & Sons, New York, 1992, Vol. 1, pp. 83–103.

23. (a) Atta-ur-Rahman, *Nuclear Magnetic Resonance Basic Principles,* Springer-Verlag, 1986, pp. 116–118. (b) J. K. M. Sanders and B. K. Hunter, *Modern NMR Spectroscopy: A Guide for Chemists,* 2nd ed., Oxford University Press, New York, 1993, Chap. 2, pp. 56–62.

24. B. Tomita and H. Ono, *J. Polym. Sci. Polym. Chem. Ed.,* **17,** 3205 (1979).

25. For a theoretical treatment of quantitative analysis of ^{13}C-NMR, see (a) S. Gillet and J.-J. Delpuech, *J. Magn. Reson.,* **38,** 433 (1980). For reviews, see (b) L. A. C. Peters and A. J. Vlietinck, *J. Pharm. Biomed.* *Anal.,* **7,** 1405 (1989); (c) J. N. Shoolery, *Prog. Nucl. Magn. Reson. Spectrosc.,* **11,** 79 (1977). Also see (d) J. K. Baker and C. W. Mayers, *Pharm. Res.,* **8,** 763 (1991). For a compilation of various NMR techniques for quantitative ^{13}C-NMR analysis, see (e) H. C. A. Hegg, in *17th Nordwegian Lipid Symposium Proceedings,* Y. Maikki and G. Lambetsen, Eds. (Scand. Forum Lipid Res. Technol.), Bergen, Norway, 1993, pp. 240–241; *Chem. Abstr.,* **121,** 229144 (1994).

26. P. M. Henrichs, J. M. Hewitt, L. J. Schwartz, and D. B. Bailey, *J. Polym. Sci. Polym. Chem. Ed.,* **20,** 775 (1982).

27. (a) E. Malmström, M. Johansson, and A. Hult, *Macromolecules,* **28,** 1698 (1995). (b) C. J. Hawker, R. Lee, and J. M. J. Fréchet, *J. Am. Chem. Soc.,* **113,** 4583 (1991).

28. W. J. Blank, *J. Coat. Tech.,* **51**(656), 61 (1979).

29. H. Schindlbauer and J. Anderer, *Angew. Makromol. Chem.,* **79,** 157 (1979).

30. B. Tomita and C.-Y. Hse, *Mokuzai Gakkaishi,* **41,** 349 (1995).

31. A. T. Nielsen, D. W. Moore, M. D. Ogan, and R. L. Atkins, *J. Org. Chem.,* **44,** 1678 (1979).

32. A. D. English, D. B. Chase, and H. J. Spinelli, *Macromolecules,* **16,** 1422 (1983).

33. K. Holmberg, *Polym. Bull.,* **11,** 81 (1984), and references therein.

34. A. G. Giumanini, G. Verardo, F. Gorassini, T. Scubla, P. Strazzolini, F. Benetollo, and G. Bombieri, *J. Chem. Soc. Perkin Trans 2,* 1771 (1995).

Note added in proof: Similar assignments of the ^{13}C NMR chemical shifts in Tables III and IV were reported by L. A. Panangema, and A Pizzi, *J. Appl. Polym. Sci.,* **59,** 2055 (1996).